Proceedings of the Liquid Metal Processing & Casting Conference 2017
Edited by: Matthew J.M. Krane, R. Mark Ward, Stuart Rudoler, Andrew J. Elliott, and Ashish Pate

CFD MODELING OF THE ELECTRODE CHANGE DURING THE ESR PROCESS

E. Karimi-Sibaki [1], A. Kharicha [1,2], M. Wu [1,2], A. Ludwig [2], H. Holzgruber [3],
B. Ofner [3], A. Scheriau [3], M. Kubin [3], and M. Ramprecht [3]

[1]Christian-Doppler Laboratory for Advanced Process Simulation of Solidification and Melting,
[2] Chair of Simulation and Modeling of Metallurgical Processes,
Montanuniversitaet of Leoben, Franz-Josef-Str. 18, A-8700 Leoben, Austria
[3] INTECO melting and casting technologies GmbH, 8600 Bruck/Mur, Austria

Keywords: Electroslag remelting (ESR), electrode change, melt rate,
numerical modeling, melt pool profile

Abstract

Nowadays, electrode change technique is necessarily used during the electroslag remelting (ESR) process for producing large ingots. A number of small electrodes are remelted in series for a large ingot. The electrode change procedure includes following steps: switching off the input power (~ 5 min), heating up the tip of new electrode to the melting temperature (~ 10 - 15 min), and increasing gradually the melt rate to reach the target value (~ 10 - 15 min). Here, a numerical investigation is performed. The interaction between the turbulent flow, heat, and electromagnetism are modeled for a large-ingot (~ 2 m in diameter) ESR process with short collar mold. Impacts of the power and melt rate interruption on the flow and thermal fields as well as solidification of the ingot during the full procedure of the electrode change are analyzed.

Introduction

Producing large heavy ingots (> 100 tons) through the electroslag remelting (ESR) is a long process that may take several days. Nowadays, the electrode change technique is effectively applied, and a number of small electrodes are re-melted in series to produce one big ingot. The entire electrode change procedure comprises three steps. Firstly, the power is switched off when a preheated electrode is prepared to be immersed into the molten slag (~ 5 min). Secondly, the electric current flows again through the system to heat the electrode tip aiming at reaching the melting temperature (~ 10 - 15 min). Finally, the electrode starts to melt and the melt rate gradually increases to reach the target melt rate (~ 10 - 15 min). Special care must be taken to avoid internal and surface defects during the full procedure for electrode change due to the power interruption in the system.

Holzgruber et al [1] reported no traceable change in the chemical composition in the ingot during the power interruption. On the other hand, Matushkina et al [2] found some defects on the surface of ingot during electrode change. Jackson et al [3] analyzed heat balances across the ingot during power interruption. They found that solidification occurred much more rapidly at the pool periphery rather than in the ingot center. They concluded that gross changes in structure and composition of ingot are not expected unless power interruption lasts for too long time. Previously, we presented a CFD model for predicting the behavior of the system during the first step of electrode change [4]. In this study, we extended the model for the full procedure of the electrode change by including all three steps. A numerical study is performed. The interaction between the turbulent flow, heat, and electromagnetic fields are taken into account. Furthermore, the model considers the effect of movement of interface between molten slag and melt pool. An ESR process with short collar mold is studied, and the behavior of system is continuously tracked during all three aforementioned steps for approximately 30 minutes. Impacts of the power and melt rate interruption on the flow and thermal fields as well as solidification of the ingot during the full procedure of the electrode change are analyzed.

Modeling

All details of the model including governing equations and related boundary conditions for the transport phenomena (e.g. flow, thermal, electromagnetic) are presented in Refs [4-5]. Thickness of the slag skin is kept constant during the whole simulation. This assumption is made according to the measurement of skin thickness during the plant trial. A uniformly thin layer (~ 5 mm) is observed

Table 1. Parameters used in our calculation.

Mater. properties	**Slag**	**Steel**	**Operation parameters**	
Density ($kg.m^{-3}$)	2440	7000	Ingot diam. (m)	1.979
Viscosity (Pa.s)	0.01	0.0062	Elec. diam. (m)	1.1
Specific heat ($J.kg^{-1}$)	1255	500-800	Ingot length (m)	1.6
Liq. therm. cond. ($W.m^{-1}.k^{-1}$)	1.5-5	25-40	Slag height (m)	0.335
Sol. therm. cond. ($W.m^{-1}.k^{-1}$)	0.5	16	RMS current (kA)	46
Therm. exp. Coeff. (K^{-1})	0.0001	0.00011	Freq. (Hz)	0.2
Liquidus temp. (K)	1715	1773	Power (MW)	2.5
Solidus temp. (K)	1598	1668		
Liq. e. cond. ($ohm^{-1}.m^{-1}$)	180	$8.8x10^5$		
Sol. e. cond. ($ohm^{-1}.m^{-1}$)	15	$8.8x10^5$		

along the whole ingot. Furthermore, all parameters used in our calculations are listed in Table 1.

Figure 1 indicates variations in melting parameters such as power (green), electric current (red), and melt rate (black) during the whole electrode change procedure. Melting parameters are kept constant before electrode change which is considered as step zero in our simulation. Then, all melting parameters drop to zero during the first step (step one) that takes approximately three minutes. Afterwards, a large amount of electric current, as well as power, is imposed to the system to heat up the tip of the new electrode in 15 minutes. The melt rate remains at zero, whereas the imposed electric current (power) decreases in stepwise. Finally, the electrode starts to re-melt at constant imposed electric current (power) at step three (~ 10 min) in which the melt rate increases in a linear manner to reach the target value.

Results and discussions

Modeling results of calculations such as electric current density (including mold current), magnetic flux density, velocity, temperature, turbulence kinetic energy, and turbulence effective thermal conductivity before electrode change at step zero were presented previously [4]. Figure 2 illustrates velocity, thermal, and solidification fields at the end of all aforementioned steps. At the end of step one (power off), the pool profile is slightly influenced near the ingot-mold interface where the cooling rate is large. However, the flow pattern is totally changed. The clock-wise rotating vortex (converging flow) disappears in the slag zone. The flow is completely driven by the buoyance force during step one that leads to counter-clock wise rotation of flow (diverging flow) in the slag. The magnitude of velocity decreases notably in the bulk with the time, whereas the flow is still strong near the mold wall due to thermal buoyancy. Furthermore, the slag becomes colder as a consequence of switching off the heat source (Joule heating). In contrast, the temperature of slag increases again at the end of step two especially under the shadow of electrode where the current density and subsequently Joule heating is high. The solidification proceeds near the slag-mold-melt pool interface during the second step. However, the flow pattern adapts gradually to the similar condition of steady state (step zero). Eventually, the flow field remains relatively unchanged during the step three. On the other hand, the temperature decreases in the slag zone because of melting droplets which carry the heat from the slag to the melt pool. Based on the simulation results, a minor impact was observed on the pool profile in the bulk of the ingot at the end of electrode change procedure. However, gross changes were observed in the solidification profile near the region of standing height.

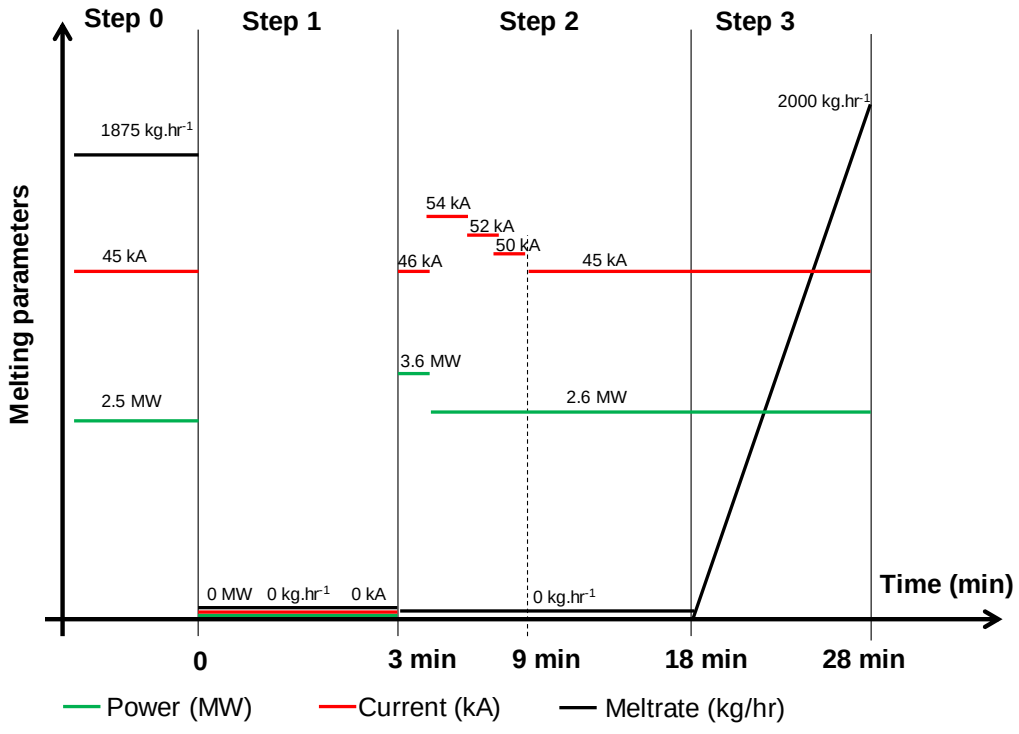

Figure 1. Melting parameters including power (green line), electric current (red line), and melt rate (black line) during the whole procedure of electrode change.

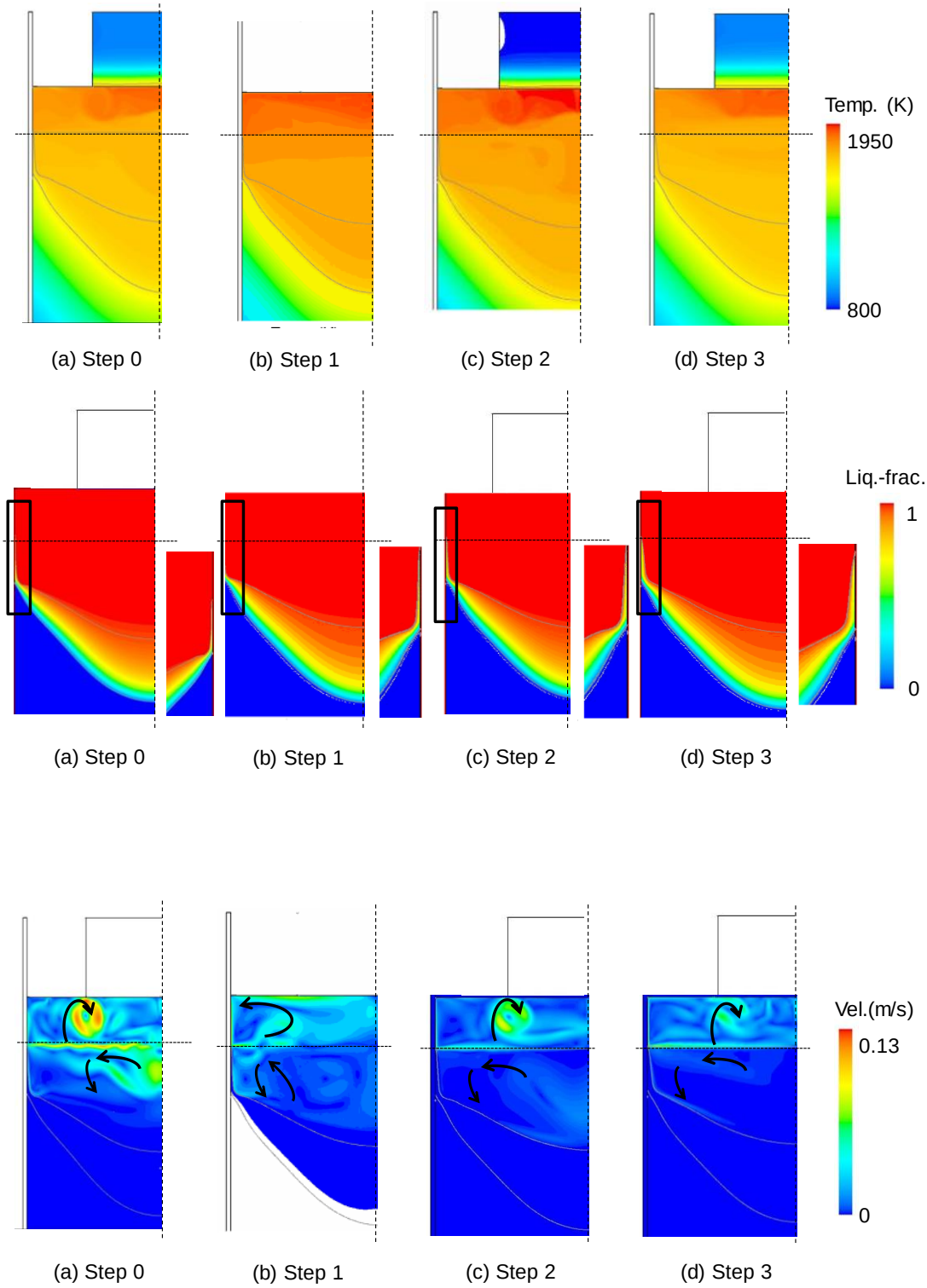

Figure 2. Snapshots of dynamic change of thermal and velocity fields as well as solidification pool profile at the end of aforementioned steps (steps 0, 1, 2, and 3) during the whole procedure of electrode change. First row shows contours of velocity fields; Second row shows contours of temperature overlaid with isolines of solid fraction; Third row shows contours of liquid fractions where a zoomed area near the standing height (liquid metal in direct contact to mold) is also illustrated.

Summary

Manufacturing large heavy ingots requires electrode change. Several small electrodes are re-melted to build a big ingot. The electrode change procedure involves three steps: (i) switching off the input power to immerse the newly preheated electrode into the slag, (ii) switching on the input power to heat up the tip of the new electrode to the melting temperature, (iii) increasing melt rate of the electrode to the target value. In this study, CFD simulation tools are used to model the whole electrode change procedure. A 2D axisymmetric computational domain is considered where the movement of slag-melt pool interface is considered. The interactions between turbulent flow, electromagnetic, and temperature fields are considered. Generally, the pool profile is an indicator of ingot internal quality. Therefore, preserving the original pool profile before and after electrode change procedure is a symptom of maintaining ingot quality. According to simulation results, changes in the pool profile in the bulk of ingot are insignificant. The gross change is observed near the standing height where liquid metal is in direct contact to the mold.

Acknowledgements

The authors acknowledge the financial support by INTECO melting and casting technologies GmbH and Austrian Federal Ministry of Economy, Family and Youth and the National Foundation for Research, Technology and Development within the framework of the Christian Doppler Laboratory for Advanced Process Simulation of Solidification and Melting.

References

[1] W. Holzgruber, C. Kubisch, and H. H. Jaeger, Neue Hütte, 1971, vol. 16, p. 606.

[2] L. I. Matushkina, M. Klyuver, L.A Dedushev, L. L. kosyrev, S.E. Volkov, and A. A. Sharapov, S.b. Tr. Tsent. Nauch-Issted. Inst Chern. Met. , in Russian, 1970, vol. 75, p. 167.

[3] R.O. Jackson, A. Mitchell, and J. Luchok, J. Vac. Sci. Tech., 1972, vol. 9 (6), p. 1301.

[4] E. Karimi-Sibaki, A. Kharicha, M. Wu, A. Ludwig, H. Holzgruber, B. Ofner, A. Scheriau, M. Kubin, M. Ramprecht, IOP Conf. Series: Materials Science and Engineering 143 (2016) 012006 DOI:10.1088/1757-899X/143/1/012006.

[5] E. Karimi-Sibaki, A. Kharicha, J. Bohacek, M. Wu, A. Ludwig, Adv. Eng. Mater., 2016, vol.18, 224-230.